Properties of some low-lying electronic states in polymethineimines and poly(2,3-diazabutadienes)

I. D. L. Albert and S. Ramasesha
Solid State and Structural Chemistry Unit, Indian Institute of Science, Bangalore 560 012, India

P. K. Das
Department of Inorganic and Physical Chemistry, Indian Institute of Science, Bangalore 560 012, India
(Received 15 October 1990)

Polymethineimines (PMI's) and poly(2,3-diazabutadienes) (PBD's) are isoelectronic with polyacetylenes (PA's), but they do not possess the electron-hole or the spatial symmetries of PA. While PMI has been synthesized, PDB still remains to be prepared in the laboratory. In this paper, we have calculated the properties of some low-lying electronic states of PMI and PDB polymers, employing a Pariser-Parr-Pople model Hamiltonian. The nitrogen-atom parameters used in the model are obtained after extensively testing them in simple nitrogen-containing molecules. The electronic states in small polymers are obtained by exactly solving the finite model Hamiltonians employing a valence-bond procedure. The energy levels and other properties of the infinite system are then obtained from extrapolations. Our studies show that the optical gap in a single strand of PMI is 2.6 ± 0.2 eV, which is very close to the single-strand PA value of 2.8 ± 0.2 eV. The gap in PDB is 3.8 ± 0.4 eV and, unlike the case for PA systems, there are no "in-gap" states in PMI or PDB. The transition dipoles to these states from the ground state as well as dipole moments in the ground state point to a nonlocal nature of the ground and excited states.

I. INTRODUCTION

Electronic properties of one-dimensional conjugated polymers isoelectronic with polyacetylenes (PA's) have become a current topic for investigation.[1–3] This spurt of interest has been triggered mainly by the extensive theoretical and experimental findings on long-chain polyenes.[4–8] Polymethineimines (PMI's) and poly(2,3-diazabutadienes) (PDB's) are two polymers isoelectronic with PA's. The PMI analogs are easily synthesized by heating polyacrylonitrile (PAN) at about 200 °C,[9] while the synthesis of PDB analogs has not yet been reported in the literature. Molecular structures of these systems are shown in Fig. 1. Polymethineimines are similar in configuration to that of the *trans*-polyenes, and PDB's that of the *cis*-polyenes. However, the electronic structures of these polymers are expected to be different from those of polyenes because the more-electron-donating nitrogen atoms now replace half the carbon atoms in the latter.

The PMI system has been theoretically investigated by Karpfen[10] ad Brédas *et al.*[11] Karpfen, employing *ab initio* crystal-orbital calculations, has obtained the optimized geometry of PMI's in the all-*trans* configuration. Brédas *et al.* have carried out band-structure calculations of PMI's using the valence-effective-Hamiltonian approach. They have reported an optical gap of $\cong 5.4$ eV in this system, which is more than twice the gap observed in all-*trans* polyacetylenes. However, it is believed that in organic semiconductors, substitution of heteroatoms having a lone pair of electrons leads to a reduction in the band gap.[12] Brédas *et al.* further conclude that there is significant σ-π interaction in PMI's leading to an overlap of the σ and the π bands. Both these calculations are, however, carried out within the mean-field approximation. While the mean-field approach provides reliable ground-state energies and geometries, it is inadequate for excited-state properties. This has been demonstrated conclusively in the case of PA's.[6,7] The presence of nitrogen atoms is expected not to change the electron-electron interactions drastically and hence a detailed investigation within correlated models with appropriate parameters is

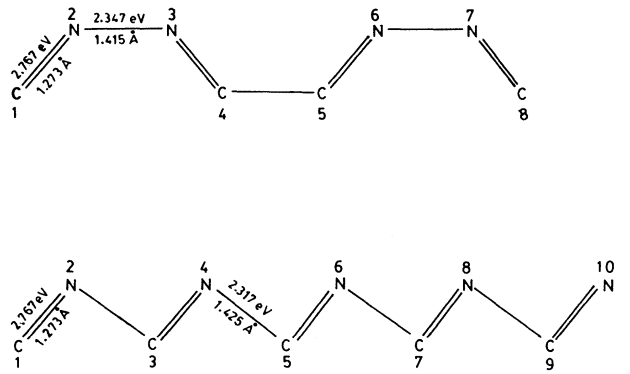

FIG. 1. Structures of polymethineimine $(—HC=N—)_x$ and poly(2,3-diazabutadiene) $H_2C=N—N=CH—CH=N—N=CH_2$ showing the bond lengths, bond angles, and the transfer integrals.

necessary to understand the low-lying states of these nitrogen-containing polymers. In this paper we have investigated the role of heteroatoms on the energies and other properties of some of the low-lying electronic states in conjugated polymers.

In the following section we introduce, in brief, the π-electron model used in these calculations and present a detailed analysis for obtaining the nitrogen-atom parameters. In the third section we discuss our results of the model exact electronic states in these polymers.

II. PARISER-PARR-POPLE (PPP) MODEL AND NITROGEN-ATOM PARAMETERS

The PPP model Hamiltonian is obtained by starting with the orbitals involved in π conjugation (usually the p_z orbitals of carbon atoms in conjugated polyenes) and then by invoking a zero-differential-overlap approximation.[13,14] This leads to a π-electron Hamiltonian in which the one-electron terms involve transfer of electrons between the nearest-neighbor (p_z) orbitals, besides the orbital energy. The interaction part of the Hamiltonian consists of an on-site repulsion term (which is the same as the parameter U in the Hubbard models) and an intersite interaction term. The latter is usually parametrized to interpolate between U for on-site interaction and e^2/r when the charged sites are far away from each other. The PPP Hamiltonian is then written as

$$\begin{aligned} H_{\mathrm{PPP}} = & \sum_{p=1}^{N} \sum_{\sigma} \varepsilon_p a_{p\sigma}^{*} a_{p\sigma} \\ & + \sum_{p=1}^{N-1} \sum_{\sigma} t_{p,p+1} (a_{p\sigma}^{*} a_{p+1,\sigma} + \mathrm{H.c.}) \\ & + \sum_{p=1}^{N} U_p \hat{n}_{p,\sigma} \hat{n}_{p,-\sigma} \\ & + \tfrac{1}{2} \sum_{1 \le q < p \le N} V_{pq} (\hat{n}_p - 1)(\hat{n}_q - 1) , \end{aligned} \tag{1}$$

where ε_p is the site energy at the pth atom, $t_{p,p+1}$ is the transfer integral, $a_{p\sigma}$ ($a_{p\sigma}^{*}$) annihilates (creates) an electron on the pth atom, n_p are the corresponding occupation-number operators, and U_p is the on-site correlation energy, which is different for carbon and nitrogen atoms. The bond angles between all successive single and double bonds are taken as 120°. Since the PPP Hamiltonian conserves the total spin of the Hamiltonian, use of the total-spin-adapted functions helps in reducing the size of the matrices as well as in labeling the states. We employ the diagrammatic valence-bond basis, which is easy to construct and to manipulate. The calculations have all been done on a Digital Equipment Corporation micro-VAX-II computer system.

The PPP parameters used in a calculation are commonly the renormalized parameters that include effects of the σ framework and not the π electrons alone. These parameters for carbon in the sp^2 hybridization are well established and are transferable from one molecule to another. The success of the PPP Hamiltonian, which only considers the π framework, lies in the fact that in large conjugated systems the excitations in the σ framework are well separated in energy from those of the π system.

The PPP parameters for heteroatoms (i.e., atoms other than carbon), however, are not well standardized. Thus the reliability of a calculation done on a system having heteroatoms depends very much on the choice of these parameters. Before undertaking a serious π-electron calculation, it is necessary to check the parameters on smaller and experimentally well-studied systems. For sp^2-hybridized nitrogen the six-membered-ring systems containing one (pyridine), two (pyrimidine and pyrazine), and three (*s*-triazine) nitrogen atoms provide an excellent testing ground since these molecules have been extensively studied experimentally[15,16] as well as theoretically. The parameters are directly taken from the literature[17] and tested within the PPP model against the experimental excitation energies of these six-membered-ring systems. The energy of the nitrogen p_z orbital is -2.96 eV relative to the carbon p_z orbital, and the difference reflects the higher effective nuclear charge experienced by the p_z orbital in the former. The on-site repulsion energy of 12.34 eV for the nitrogen p_z orbital is 1.08 eV higher than that of the carbon p_z orbital, which has a less compact p_z orbital. The intersite interaction potential is given by Ohno's familiar expression[18]

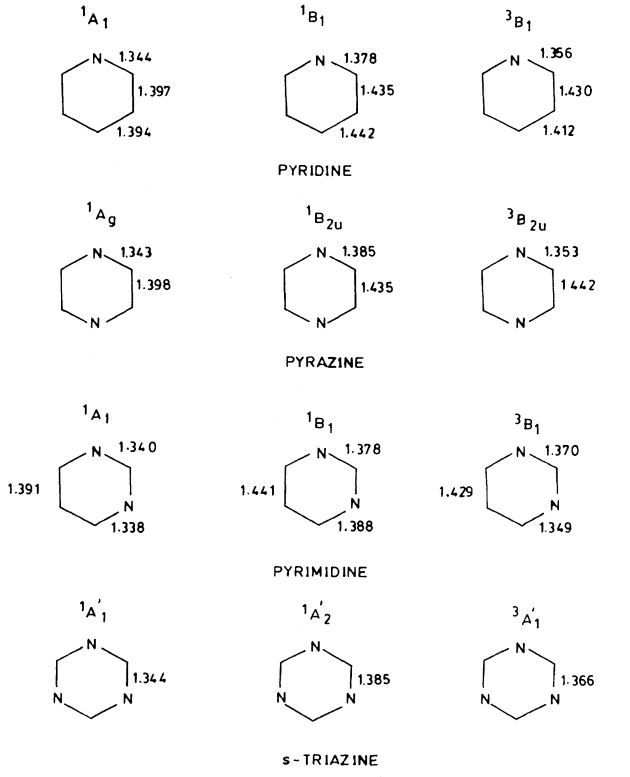

FIG. 2. Optimized geometry of pyridine, pyrazine, pyrimidine, and *s*-triazine in the two low-lying singlets and the lowest triplet. The labeling of the states is also indicated.

TABLE I. Vertical excitation energies of a few low-lying singlets and triplets of pyridine, pyrazine, pyrimidine, and *s*-triazine (1,3,5,-triazine) in both the optimized and the unoptimized geometry. The experimental excitation gaps (as quoted in Ref. 19) are given in parentheses.

	Vertical excitation energies					
	Singlet		Triplet		*S-S* gap for optimized	*S-T* gap for optimized
Molecule	State	Energy	State	Energy	geometry	geometry
Pyridine	$^1A_1$	0.0	$^3B_1$	3.690		4.019
	$^1B_1$	4.329	$^3A_1$	4.204	5.066 (4.94)	
	$^1B_2$	5.551				
	$^1A_2$	6.996				
Pyrazine	^1A_g	0.0	$^3B_{2u}$	3.728		4.021
	$^1B_{2u}$	4.2457	^3A_u	4.728	5.058 (4.77)	
	$^1B_{3u}$	5.670				
	^1A_u	7.194				
Pyrimidine	$^1A_1$	0.0	$^3B_1$	4.014		4.449
	$^1B_1$	4.5991	$^3B_1$	4.397	5.478 (5.40)	
	$^1B_2$	5.669				
	$^1A_2$	7.020				
s-triazine	$^1A_1'$	0.0	$^3A_1''$	4.461		4.865
	$^1A_2'$	5.014	$^3A_1''$	5.837	5.778 (5.58)	
	$^1A_2''$	5.829				
	$^1A_1''$	7.357				

$$V_{ij}=14.397\times\{[28.794/(U_i+U_j)]^2+r_{ij}^2\}^{-1/2}\ , \quad (2)$$

where U_i is the Hubbard on-site population integral in electron volts on site i and r_{ij} is the distance in angstroms between the sites i and j. The C-N distances and the molecular geometries in the ground state of these molecules correspond to those quoted in the literature.[19,20] Several exact PPP vertical excitation energies for these molecules are given in Table I. The energies of the low-lying states are rather insensitive to changes in U_N as well as the nitrogen orbital energy. The experimental excitation energies in each case are about 0.5 eV higher than the vertical excitation energies. The prediction of a lower excitation energy in pyrazine, compared with that of pyridine and pyrimidine, is a satisfactory feature of these calculations. The ground-state dipole moments are, however, smaller than the experimentally observed quantities.

Since the excitation energies are rather insensitive to the site energies as well as repulsion energies within reasonable ranges of these parameters, the only parameter that must be included in the PPP model is the geometry of the molecule in various excited states. Optimized geometries for some of the excited states of these molecules are known and we incorporate these geometries in our calculations as well. The transfer integrals are calculated for the new geometry using the relation[21]

$$t_{p,q}=-2.40+3.20(r_{p,q}-1.397) \quad (3)$$

and replacing $r_{p,q}$ with appropriate equilibrium bond distances in the given electronic state. The new geometries also change the intersite interaction energies in a given configuration. The excitation energies corresponding to these relaxed geometries are shown in Table I and the optimized geometries for the excited states for each of the molecules are shown in Fig. 2. We find that the calculated excitation energies are now in very good agreement with experiments, except in the case of pyrazine. The excitation energy in pyrazine is larger than the experimen-

TABLE II. Transition dipole moments (in debyes) and dipole moments (in debyes) of the first four low-lying states of pyridine, pyrazine, pyrimidine, and *s*-triazine.

Molecule	μ_{G-1}	μ_{G-2}	μ_{G-3}	μ_G	μ_1	μ_2	μ_4
Pyridine	2.661	1.038	8.348	1.445	1.286	2.447	4.091
Pyrazine	4.763	2.697	0.003	0.0	0.0	0.0	0.0
Pyrimidine	2.858	1.324	7.132	1.652	1.826	2.682	4.139
s-triazine	0.0	0.0	8.624	0.0	0.0	0.0	1.486

tal value by $\cong 0.3$ eV. However, unlike the results of earlier calculations, where the optical gap in pyrazine was predicted to be higher than in pyridine, our value is slightly smaller than that of pyridine and pyrimidine. It is likely that a better optimized geometry in case of pyrazine would lead to a closer agreement with experiment.

Our calculations predict energies of many low-lying singlets and transition dipole moments to these states from the ground state (Table II). In each case, however, geometry optimization has to be carried out before comparing theoretical calculations with experimental results. Also reported here are singlet-triplet and triplet-triplet gaps and it would be interesting to compare these quantities with experimental results, when the latter become available. All our calculations exclude the nitrogen σ-lone-pair electrons and thus cannot account for the n-π^* transitions. The good agreement between experimental data and the PPP calculations on the six-membered-ring compounds containing nitrogen atom(s) in π conjugation suggests that the PPP parameters used by us are appropriate for the nitrogen p_z orbital in the sp^2-hybridized state.

The PMI and PDB polymers differ from the polyenes in other computationally significant ways, besides the differences in the parameters. The presence of heteroatoms leads to a breakdown of the alternation or electron-hole symmetry since all the p_z orbitals are now not equivalent. Also, unlike the all-*trans* and -*cis* polyenes, these polymers do not possess any spatial symmetries. The only good quantum number in the system is therefore the total spin and no other labels exist for the electronic states. The absence of these symmetries leads to matrices whose order is $\cong 4$ times the order of the matrices encountered in polyene chains with same number of atoms, and the computational effort also correspondingly increases. The largest systems dealt with are the 12-atom PMI and PDB systems that span a singlet space of dimensionality 226 512.

III. LOW-LYING STATES IN PMI AND PDB

We have carried out exact PPP electronic-energy calculations on PMI and PDB systems with up to 12 atoms (six nitrogen and six carbon atoms) in the chain. The actual geometry and the transfer parameters used in the calculations are shown in Fig. 1. The energies of the ground and three excited states in PDB and PMI polymers have been obtained. In addition, the dipole moments and the transition dipoles to each of the states from their respective ground states are calculated. While full configuration-interaction (CI) calculations lead to size-consistent state energies, thus allowing proper extrapolations to the infinite-chain-length limit; to improve convergence in extrapolations of the optical gaps, we have also calculated the optical gaps in these polymer chains with cyclic boundary conditions and have used them in the least-squares fits. The cyclic boundary condition introduces an extra transfer integral between the end atoms in the chain, without changing the geometry of the molecule.

Presented in Table III are the excitation energies of PMI and PDB and polyenes (for comparison). We note that for finite chains of PMI, the lowest-energy excitations are always at an energy lower than those for the corresponding polyenes, although they are slightly higher than the two-photon excitation energies of the polyenes. The extrapolated optical gap (Fig. 3) for PMI's is 2.68 ± 0.2 eV, which is very close to the polyene value of 2.8 ± 0.2 eV.[7] The estimate of error in case of PMI is given by the two limits to which excitation energies in the chains and the $4n$ and $4n+2$ atom (n is a positive integer) cyclic systems extrapolate. The conjugated $4n$ cyclic systems have a lower excitation energy than the $4n+2$ cyclic systems. In the noninteracting limit of the $4n$ systems the highest occupied molecular orbitals are degenerate and hence partially occupied in the alternant systems leading to zero optical gap. This degeneracy is, however, lifted by the nonequivalence of the C and N atoms even in the Hückel picture. The $4n+2$ systems, however, have a finite gap in the homoatomic case and the gap increases by the introduction of the heteroatoms. The excitation energies in the interacting limit reflect these differences between the $4n$ and $4n+2$ systems for small n by approaching the infinite-polymer value from below and above, respectively (Fig. 3). The chain excita-

TABLE III. Low-lying singlet excitation energies (eV) of polyenes (PA's), PMI's and PDB's (PDB-6 and PDB-10 do not exist) for different chain lengths. The ground-state energy is taken as zero in each case and the excitation energies are given in increasing order of their energies.

System	4	6	8	10	12
PA	5.361[a]	4.382[a]	3.775[a]	3.391[a]	3.137[a]
	5.821[b]	5.046[b]	4.561[b]	4.207[b]	3.830[c]
	9.308[c]	5.355[c]	4.718[c]	4.234[c]	4.001[b]
PMI	5.462	4.573	4.082	3.802	3.637
	6.848	5.979	5.377	4.974	4.624
	7.685	6.079	5.423	4.979	4.698
PDB	5.672		4.582		4.129
	6.296		4.769		4.222
	8.239		5.870		

[a] $2\,^1A_g^2$.
[b] $1\,^1B_u^-$.
[c] $1\,^1B_u^+$.

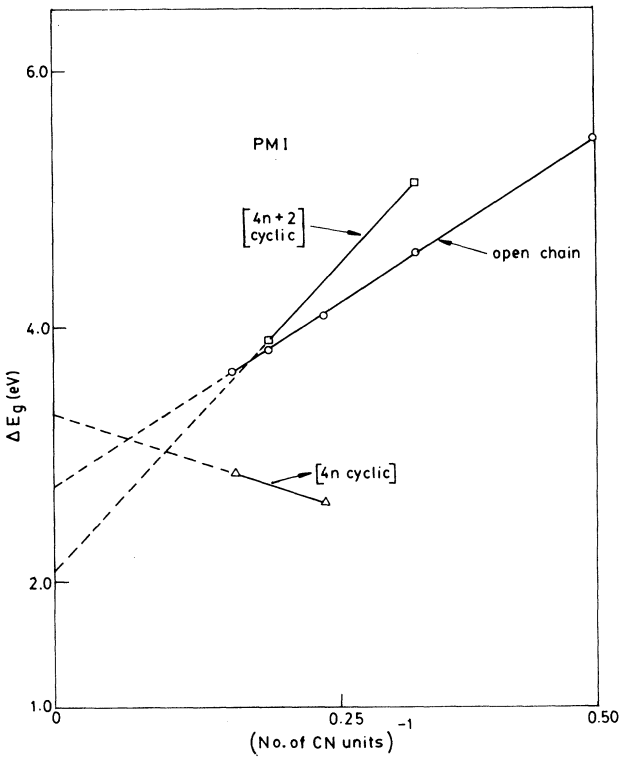

FIG. 3. Optical gap (in eV) of the open chain, $4n$ and $4n+2$ cyclic PMI systems as a function of the inverse of the number of CN units.

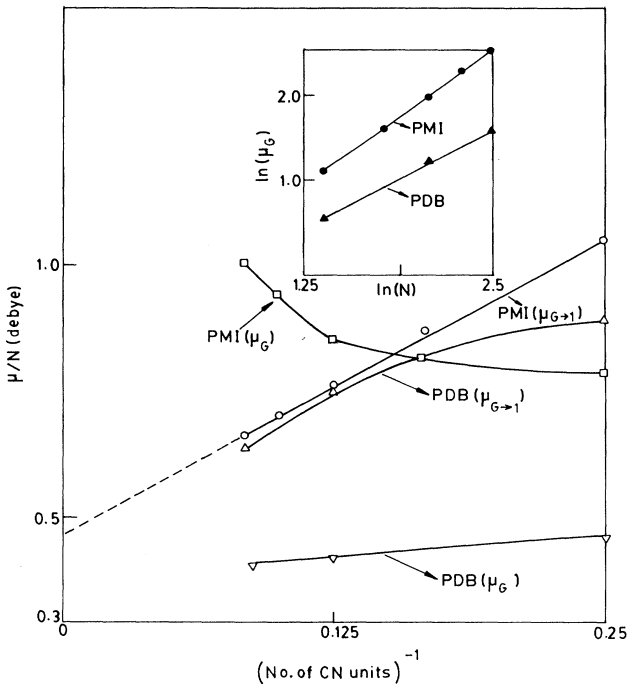

FIG. 4. Dipole moments (μ_G) and transition dipole moments to the lowest excited state ($\mu_{G\to 1}$) per CN unit as a function of the inverse of the number of CN units in PMI and PDB systems. Inset gives a log-log plot of the ground-state dipole moment as a function of the system size.

tion energies extrapolate to a value that lies approximately midway between the extrapolated values for the $4n$ and $4n+2$ systems, thereby lowering the error bars placed for the infinite polymer. This gap is considerably larger than the extrapolated lowest-energy two-photon gap in polyenes with the latter being nearly half the one-photon gap in those systems. The transition dipole moment and the dipole moment in the ground state per CN unit are also plotted as a function of system size (Fig. 4). The transition dipole moment per unit cell extrapolates to a value of 0.47 D in the infinite-polymer limit. The finite value to which this quantity extrapolates indicates that the optical excitation is nonlocal. The dipole moment per unit cell in the ground state increases with increasing system size in a power-law behavior with an exponent of $\cong 1.27$. The large dipole moment in the ground state shows that the charge separations in the ground state are not locally confined. The optical gap that we have obtained is considerably smaller than the gap that Brédas and co-workers have reported on the basis of their valence-effective-Hamiltonian calculations. They attributed the high energy gap to significant mixing of the σ and π bands. While our calculations do not explicitly take into account the σ orbitals, we believe that the extent of σ-π mixing in these systems is smaller than in polyenes. The nitrogen-atom parameters for both the orbit-

TABLE IV. The magnitude of transition dipole moments (in debyes) and dipole moments (in debyes) for the first few low-lying states of PMI's and PDB's.

Molecule	$\mu_{G\to 1}$	$\mu_{G\to 2}$	$\mu_{G\to 3}$	μ_G	μ_1	μ_2	μ_3
PMI-4	4.19	3.54	0.17	3.03	2.95	0.99	1.26
PMI-6	5.17	4.63	0.94	4.99	6.20	9.09	5.99
PMI-8	6.09	5.35	1.87	7.20	8.71	12.6	9.26
PMI-10	7.02	6.38	6.03	9.59	11.8	16.6	16.0
PMI-12	8.00	0.90	6.84	12.1	13.9	13.1	10.2
PDB-4	3.56	1.08	3.86	1.86	2.27	0.66	1.88
PDB-8	6.01	0.60	1.00	3.40	7.06	5.52	7.07
PDB-12	7.67	0.58		4.92	9.99	8.46	

al energy and the on-site correlation energy are larger than for the carbon atom in sp^2 hybridization, due to the larger effective nuclear charge that results in more compact orbitals. It is by now well established that the pure π-electron models that include electron-electron interactions satisfactorily explain the electronic spectra of conjugated homoatomic systems. Thus the σ excitations are well separated from the π excitations in the homoconjugated systems. The nitrogen parameters corresponding to more compact σ orbitals should further increase the σ-π separability in these systems.

The optical gap of the PDB polymers (Fig. 5) in the infinite-chain-length limit is 3.77 ± 0.4 eV. The extrapolated optical gap in PDB chains is less accurate because only three polymers exist, with the total number of atoms in the chain being ≤ 12 atoms. However, the optical gap in PDB is clearly larger than the optical gap in PMI or PA. We also find that the transition dipole moments to the first excited state as well as the dipole moment in the ground state, in the PDB polymers, are smaller than in the PMI polymers. The size dependence of the dipole moment is also weaker than in PMI's. The exponent for the size dependence of the dipole moment in the ground state in PDB's is $\cong 0.88$ (Fig. 4). This implies that the electrons are more localized in PDB's in these states, when compared with the corresponding states of PMI polymers.

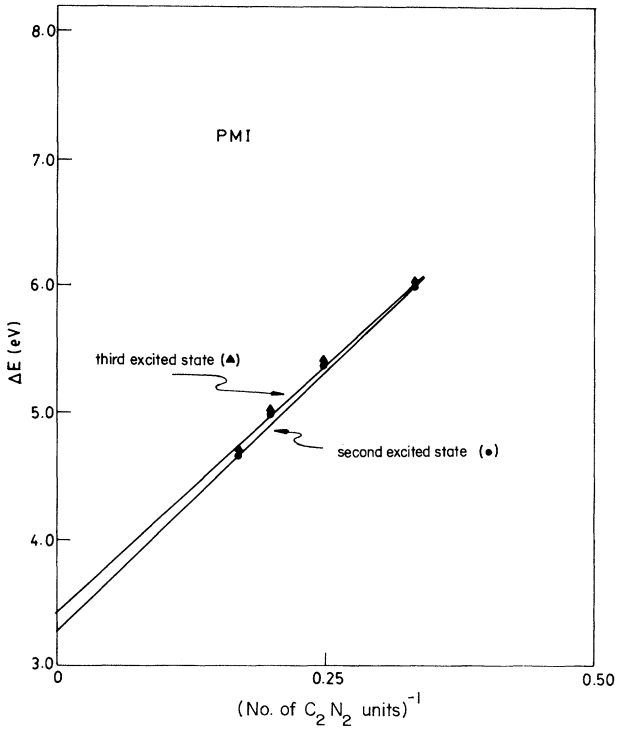

FIG. 6. Excitation gaps (in eV) to the second and third excited states of PMI's as a function of the inverse of the number of CN units.

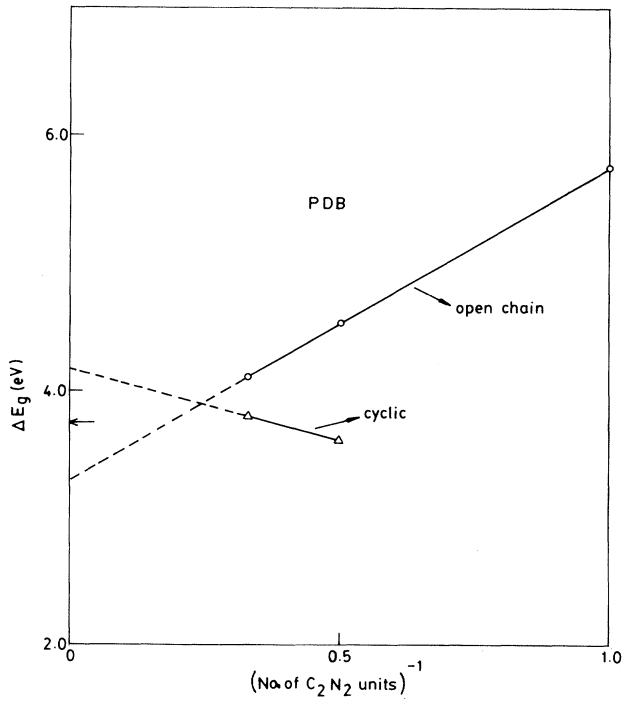

FIG. 5. Optical gap (in eV) of the open chain and the cyclic PDB systems as a function of the inverse of the number of C_2N_2 units. The arrow indicates the average gap to which the two straight lines extrapolate.

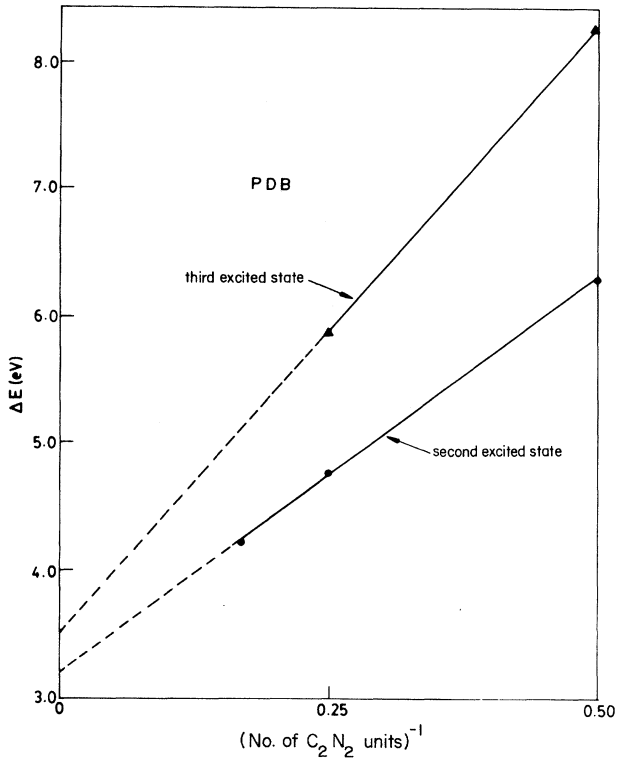

FIG. 7. Excitation gaps (in eV) to the second and third excited states of PDB's as a function of the inverse of the number of C_2N_2 units.

The higher excitation energies in PDB and PMI polymers are shown as a function of the inverse system size in Figs. 6 and 7. In PMI's the second and third excitation energies are very close to each other but well separated from the optical gap (Fig. 3). However, in PDB's the second excitation has an energy very close to the optical gap but the third excitation is well separated from these lower-energy excitations.

Presented in Table IV are the dipole moments and the transition dipoles for transitions from the ground state for the PMI and PDB polymers with up to 12 atoms. While the excitation energies show a smooth dependence on the system size (Figs. 6 and 7), the dipole moments in the excited states, as well as the transition dipole moments to the excited states, do not show a smooth dependence on system size, especially for the higher states, as seen from Table IV. This is due to the fact that the nature of the states, in terms of the charge distributions, changes with increasing system size. The number of covalent states sharply increases as we go to larger systems and, because of the lower correlation energy, a larger number of these states will have lower energies than the ionic states. This is reflected in the smaller dipole moments in the PMI system of 12 atoms compared with those of PMI-10 for the second and the third excited states.

The present calculations, which are based on an exact solution of the interacting π-electron models using reliable nitrogen-atom parameters, show that the PMI polymers have an optical gap very close to that of PA's. The experimental gap is expected, as in the case of PA's to be red shifted due to interchain interactions. However, unlike the case for polyenes, there will be no "in-gap" states in PMI's since the latter lack the symmetries that are present in polyenes. The PDB polymers have a much larger optical gap than either PMI's or PA's. A comparison of the PDB and PMI polymers suggests that any mismatch in polymerization leading to a C-N-N-C type of linkage will lead to states above the gap. The excitations in PDB's are more localized than in PMI's as seen from the dipole and transition dipole moments. In PMI's the second and third excitations are nearly degenerate and are well separated from the optical gap, while in PDB's the optical gap and the second excitation occur at nearly the same energies and third excitation is well separated from these two.

ACKNOWLEDGMENTS

One of the authors (I.D.L.A.) is grateful to the Council for Scientific and Industrial Research, India (CSIR), for financial support.

[1]J. L. Brédas, in *Electronic Properties of Polymer and Related Compounds,* edited by H. Kuzmany, M. Mehring, and S. Roth (Springer, Berlin, 1985), p. 166.
[2]M. Kertesz, Adv. Quantum Chem. **15**, 161 (1982).
[3]T. Takekoshi, Adv. Polym. Sci. **94**, 1 (1990).
[4]M. F. Granville, G. R. Holtom, and B. E. Kohler, J. Chem. Phys. **72**, 4671 (1980).
[5]K. L. D'Amico, C. Manos, and R. L. Christiansen, J. Am. Chem. Soc. **102**, 1777 (1980).
[6]S. Ramasesha and Z. G. Soos, J. Chem. Phys. **80**, 3278 (1984).
[7]Z. G. Soos and S. Ramasesha, Chem. Phys. Lett. **101**, 34 (1983).
[8]Z. G. Soos and S. Ramasesha, Phys. Rev. B **29**, 5410 (1984).
[9]D. Wohrle, Tetrahedron Lett. **22**, 1969 (1971).
[10]A. Karpfen, Chem. Phys. Lett. **64**, 299 (1979).
[11]J. L. Brédas, B. Themans, and J. M. Andre, J. Chem. Phys. **78**, 6137 (1983).
[12]Yong-Sok Lee and M. Kertesz, J. Chem. Phys. **88**, 2609 (1988).
[13]R. Pariser and R. G. Parr, J. Chem. Phys. **21**, 466 (1953).
[14]J. Pople, Trans. Farad. Soc. **49**, 1375 (1953).
[15]F. Pang, P. Pulay, and J. E. Boggs, J. Mol. Struct. **88**, 79 (1982).
[16]J. Sanchez-Marin and J. P. Malrieu, J. Phys. Chem. **89**, 978 (1985).
[17]R. L. Flurry, Jr., *Molecular Orbital Theories of Bonding in Organic Molecules* (Dekker, New York, 1968).
[18]K. Ohno, Theor. Chim. Acta **2**, 219 (1964).
[19]A. Warshel and A. Lappicirella, J. Am. Chem. Soc. **103**, 4464 (1981).
[20]J. Sanchez-Marin and J. P. Malrieu, J. Am. Chem. Soc. **107**, 1985 (1985).
[21]L. R. Ducasse, T. E. Miller, and Z. G. Soos, J. Chem. Phys. **76**, 4094 (1982).